

# Multifaceted aerosol effects on precipitation

Received: 21 December 2021

Accepted: 7 June 2024

Published online: 9 August 2024

 Check for updates

Philip Stier<sup>1</sup>✉, Susan C. van den Heever<sup>2</sup>✉, Matthew W. Christensen<sup>1,3</sup>, Edward Gryspeerdt<sup>4</sup>, Guy Dagan<sup>1,5</sup>, Stephen M. Saleeby<sup>2</sup>, Massimo Bollasina<sup>6</sup>, Leo Donner<sup>7</sup>, Kerry Emanuel<sup>8</sup>, Annica M. L. Ekman<sup>9</sup>, Graham Feingold<sup>10</sup>, Paul Field<sup>11,12</sup>, Piers Forster<sup>13</sup>, Jim Haywood<sup>12,14</sup>, Ralph Kahn<sup>15</sup>, Ilan Koren<sup>16</sup>, Christian Kummerow<sup>2</sup>, Tristan L'Ecuyer<sup>17</sup>, Ulrike Lohmann<sup>18</sup>, Yi Ming<sup>7,19</sup>, Gunnar Myhre<sup>20</sup>, Johannes Quaas<sup>21</sup>, Daniel Rosenfeld<sup>5</sup>, Bjorn Samset<sup>20</sup>, Axel Seifert<sup>22</sup>, Graeme Stephens<sup>23</sup> & Wei-Kuo Tao<sup>24</sup>

Aerosols have been proposed to influence precipitation rates and spatial patterns from scales of individual clouds to the globe. However, large uncertainty remains regarding the underlying mechanisms and importance of multiple effects across spatial and temporal scales. Here we review the evidence and scientific consensus behind these effects, categorized into radiative effects via modification of radiative fluxes and the energy balance, and microphysical effects via modification of cloud droplets and ice crystals. Broad consensus and strong theoretical evidence exist that aerosol radiative effects (aerosol–radiation interactions and aerosol–cloud interactions) act as drivers of precipitation changes because global mean precipitation is constrained by energetics and surface evaporation. Likewise, aerosol radiative effects cause well-documented shifts of large-scale precipitation patterns, such as the intertropical convergence zone. The extent of aerosol effects on precipitation at smaller scales is less clear. Although there is broad consensus and strong evidence that aerosol perturbations microphysically increase cloud droplet numbers and decrease droplet sizes, thereby slowing precipitation droplet formation, the overall aerosol effect on precipitation across scales remains highly uncertain. Global cloud-resolving models provide opportunities to investigate mechanisms that are currently not well represented in global climate models and to robustly connect local effects with larger scales. This will increase our confidence in predicted impacts of climate change.

Less than 3% of water on Earth sustains life. Precipitation is the most important mechanism delivering fresh water from the atmosphere to the surface. Although climate change discussions are commonly framed in terms of global temperature change, precipitation changes drive actual impacts of climate change on the planet<sup>1,2</sup>.

A substantial body of literature exists describing the impact of greenhouse gas- (GHG-) induced warming on precipitation, and the concepts are well understood<sup>2,3</sup>. By contrast, the uncertainty

regarding aerosol (nano- to micrometre-sized particles suspended in air of anthropogenic or natural origin) effects on precipitation (APEs) remains large. Many hypotheses describe APEs on the basis of radiative and cloud microphysical arguments. Some are included in current climate models; others are not (compare Fig. 1 and Table 1). Large uncertainty remains regarding the underlying mechanisms and relative importance of proposed effects across spatial and temporal scales.

A full list of affiliations appears at the end of the paper. ✉e-mail: [philip.stier@physics.ox.ac.uk](mailto:philip.stier@physics.ox.ac.uk); [Sue.vandenHeever@colostate.edu](mailto:Sue.vandenHeever@colostate.edu)

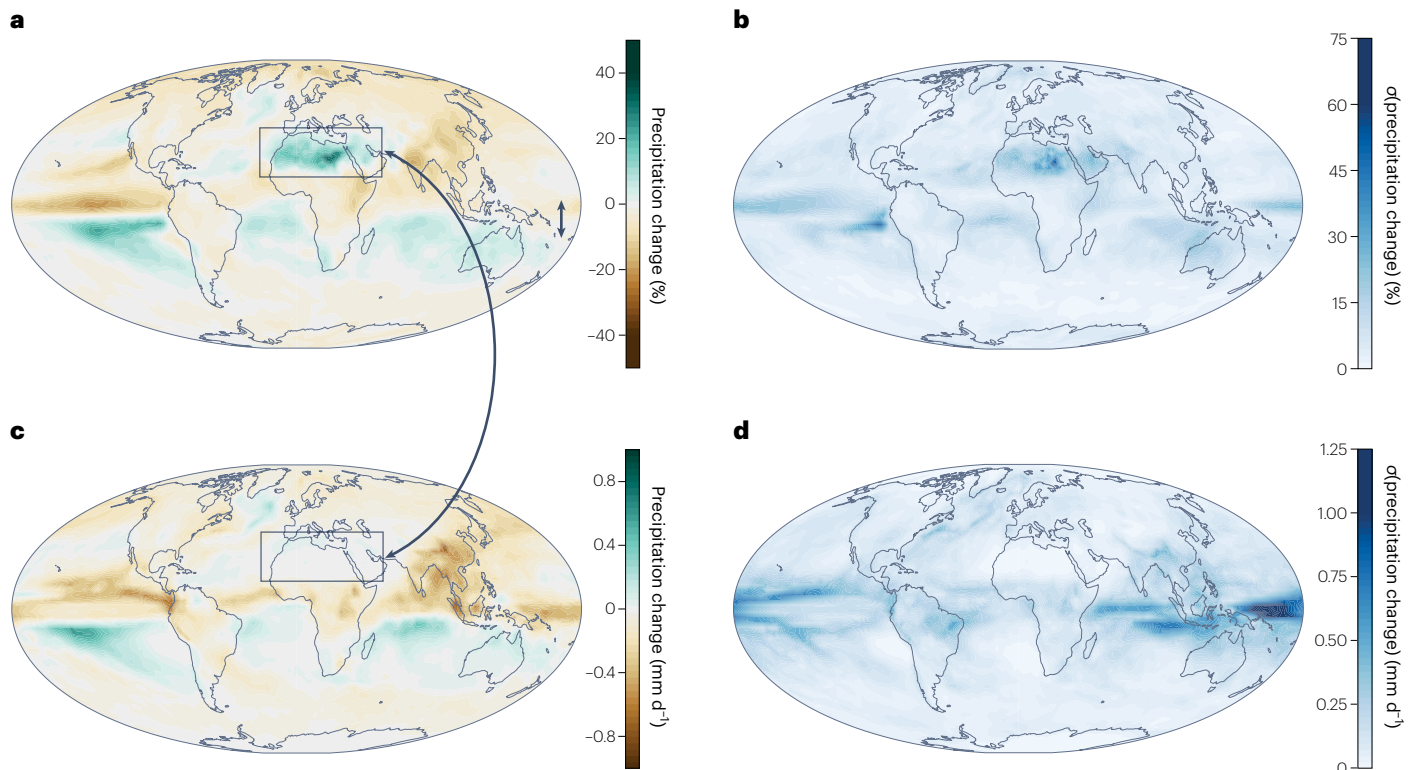


**Fig. 1 | Precipitation change due to anthropogenic aerosol in current climate models. a–d.** Climate model-simulated relative (a) and absolute (c) precipitation changes (%) due to anthropogenic aerosol from the Coupled Model Intercomparison Project Phase 6 (CMIP6) Detection and Attribution Model Intercomparison Project (DAMIP)<sup>203</sup> (difference between last 30 years

of present-day *hist-aer* minus pre-industrial *picontrol* control simulations) and the corresponding multimodel standard deviations (b,d), respectively. Note the substantial differences between relative (a) and absolute (c) precipitation changes, highlighted in the boxes over northern Africa and the Middle East.

This Review Article builds on the results of an expert workshop held under the auspices of the Global Energy and Water Cycle Exchanges (GEWEX) Aerosol Precipitation (GAP) initiative<sup>4</sup>. It critically reviews the current evidence and scientific consensus (in the authors' view) for APEs and their proposed mechanisms. To facilitate this assessment, we categorize mechanisms according to their degree of scientific support: category A, strong evidence/broad consensus; category B, some evidence/limited consensus; category C, hypothesized/no consensus.

## The physical mechanisms of aerosol effects on precipitation

The physical drivers of APEs can be categorized into (1) radiative effects via modification of radiative fluxes and the energy balance, which occur due to aerosol scattering and absorption, and (2) modification of cloud radiative properties by microphysical effects via modification of cloud droplet and ice crystal number, size and morphology, which can affect growth to precipitation-size particles, as well as latent heat from phase changes (enthalpy of vaporization or fusion). All these effects can induce dynamical feedbacks across scales.

In addition to this mechanistic (bottom up) view, conservation laws provide a complementary (top down) perspective: conservation of energy constrains global mean precipitation<sup>5–7</sup> as changes in latent heat of condensation ( $L$ ) associated with precipitation changes ( $dP$ ) have to be compensated by opposite changes in net column-integrated cooling ( $dQ$ ) through adjustment of net surface sensible heat ( $dF_{SH}$ ) and radiative ( $dF_{RAD}^{SUR}$ ) fluxes or top-of-atmosphere radiative fluxes ( $dF_{RAD}^{TOA}$ ), and vice versa. At smaller spatial scales, net latent heating associated with precipitation changes can also be balanced through divergence of dry static energy<sup>5,8–10</sup> ( $d(\nabla \cdot \mathbf{u}s)$ ) (column integrated, with  $\mathbf{u}$  horizontal velocity, neglecting changes in energy and liquid or solid water storage and kinetic energy transport), as illustrated in Fig. 2:

$$LdP = dQ + d(\nabla \cdot \mathbf{u}s) \quad (1)$$

Conservation of water provides additional constraints. In the global mean and for sufficiently long time scales, precipitation  $P$  must be balanced by evaporation  $E$  so  $P - E = 0$ . On smaller spatial scales, moisture ( $q_v$ ) flux convergence can compensate for imbalances in  $P - E$  so that:

$$dP - dE = -d(\nabla \cdot \mathbf{u}q_v) \quad (2)$$

This implies the existence of breakdown scales of budgetary constraints on precipitation—a scale below which energy and water budget constraints on precipitation do not strictly apply due to efficient horizontal transport<sup>11</sup>. In the extra-tropics, this scale is expected to be related to the first baroclinic Rossby radius of deformation ( $L = \frac{NH}{f_0} \approx 1,000$  km, where  $N$  is the Brunt–Väisälä frequency,  $H$  is the scale height and  $f_0$  is the Coriolis parameter). This latitudinally dependent precipitation constraint on aerosol perturbations implies varying effects in the tropics and extra-tropics (Fig. 3). Even for regional aerosol perturbations, energetic constraints apply to the global mean. Reductions in surface insolation and atmospheric heating by aerosol absorption decrease global mean precipitation in both simulations, with teleconnections in the tropical simulation.

Evidence from climate models shows that localized aerosol absorption could affect tropical precipitation over thousands of kilometres<sup>12</sup>. Similar scale arguments apply to the moisture budget, with limitations on moisture convergence constraining the susceptibility of regional APEs<sup>13</sup>. The combination of energy and water budget constraints (smallest closure scale) yields a characteristic scale for regional precipitation responses<sup>11</sup> of 3,000 km to localized aerosol perturbations, similar to scales of weather systems<sup>14</sup>.

**Table 1 | Assessment of the effect of increasing aerosol on precipitation**

Physical driver of aerosol effect on precipitation	Pathway	Expected effect on mean	Expected effect on intensity distribution	Included in CMIP6 climate models?	Scientific consensus category
Surface energy budget	Radiative	Decrease	Uncertain	Yes	A
Atmospheric diabatic heating	Radiative	Decrease	Uncertain	Yes	A
Semi-direct effects	Radiative	Uncertain	Uncertain	Yes	B
Regional-scale and monsoon dynamics	Radiative	Regional shifts	Uncertain	Yes	B
Sea surface temperature patterns	Radiative	Regional shifts	Uncertain	Yes	B
Hemispheric asymmetry	Radiative	Regional shifts	Neutral	Yes	A
CCN-mediated effects on stratiform liquid clouds	Microphysical	Neutral	Uncertain	Yes (substantial uncertainties)	B
CCN-mediated effects on shallow convection	Microphysical	Uncertain	Broaden	No	B
CCN-mediated effects on deep convection	Microphysical	Uncertain	Broaden	No	C
INP-mediated effects	Microphysical	Uncertain	Uncertain	No (in most models)	C

It is important to note that this budgetary framework does not provide direct constraints on precipitation intensity distributions, despite constraints on its mean. APEs could invoke an additional feedback mechanism through the radiative effects of atmospheric humidity and clouds<sup>15</sup>. Combined, energy and moisture budget constraints can provide physical mechanisms underpinning the ‘buffering’ of APEs<sup>16</sup> in equilibrium conditions, which is also related to radiative–convective equilibrium concepts<sup>17–19</sup>.

APEs can be decomposed into adjustments due to instantaneous atmospheric net diabatic heating, including rapid adjustments of the vertical structure of water vapour, temperature and clouds (hours to days), and a slower response mediated by surface temperature changes<sup>6,20,21</sup> defined as ‘hydrological sensitivity’<sup>9,22</sup>. Due to difficulties in separating fast surface temperature changes (days to months) from rapid adjustments in climate models, these are commonly considered jointly<sup>20,21</sup>.

Finally, both radiative and microphysical effects and associated changes to the regional energy balance can lead to dynamical effects and regional circulation changes with concomitant changes in precipitation<sup>23,24</sup>.

We now discuss each potential mechanism underlying APEs and assess their evidence and scientific consensus.

## Radiative effects

### Surface energy budget

Aerosol–radiation interactions (ARIs) and aerosol–cloud interactions modulate radiative surface fluxes and, consequently, sensible and latent heat fluxes. These effects generally reduce surface insolation, decreasing surface evaporation, which has been linked to a ‘spin down’ of the hydrological cycle<sup>25</sup>. This is corroborated by the observed precipitation response to ARIs following major volcanic eruptions, showing substantial decreases in precipitation over land and river discharge into ocean<sup>26,27</sup>. (Near-surface absorbing aerosol can enhance precipitation through diabatic heating, even when surface sensible heat fluxes are reduced<sup>28</sup>.) Energetically, the net-negative total ARIs<sup>29</sup> reduce the global mean temperature, atmospheric water vapour and associated long-wave emissions, which is compensated by reductions in precipitation and associated latent heat: climate models show that negative aerosol radiative forcing masks almost all temperature-driven GHG effects on precipitation over land up to present (with GHG effects dominating the future)<sup>9,30,31</sup>. However, such radiative arguments cannot be decoupled from dynamical feedbacks, as shown in the following.

That ARIs reduce global precipitation through changes in surface temperature and surface fluxes builds on our physical understanding of the energy budget, is supported by observational evidence<sup>32</sup> and

is reproduced by climate models. We assess this effect as category A, supported by strong evidence and broad scientific consensus, although magnitudinal uncertainties remain.

The following two mechanisms could be combined as aerosol absorption effects, but we retain the mechanistic separation prevailing in existing literature.

### Atmospheric diabatic heating

Atmospheric diabatic heating by aerosol absorption creates local energetic imbalances. To ensure energy conservation, this is compensated by reductions in latent heat release through precipitation, by rapid adjustments of net surface or top-of-atmosphere fluxes or, on smaller scales or in the tropics<sup>11,33</sup>, through divergence of dry static energy<sup>8,34</sup>. The energetic framework provides a useful tool to diagnose APEs<sup>9,21,28,34,35</sup> and can explain the contrasting behaviours of absorbing and non-absorbing aerosols<sup>21,36</sup>.

That diabatic heating of absorbing aerosol reduces global mean precipitation is consistent with our physical understanding of the energy budget, is reproduced by climate models but builds on limited observational evidence. We therefore assess this effect as category A, supported by strong evidence and broad scientific consensus but with remaining magnitudinal uncertainties.

### Semi-direct effects

Semi-direct effects<sup>9,37–40</sup> are rapid adjustments associated with aerosol absorption affecting the vertical temperature and humidity structure, with potential effects on clouds and precipitation. These effects are generally accompanied by corresponding surface flux changes (compare Atmospheric diabatic heating). Elevated layers of absorbing aerosol can modify lower-tropospheric static stability and sub-tropical inversion strength<sup>39,41</sup>, suppressing boundary layer deepening and concomitant entrainment<sup>42</sup>. Although the focus has been on shallow clouds<sup>43</sup>, the impact on deep convection and associated precipitation has been demonstrated in cloud-resolving models (CRMs), revealing a complex diurnal cycle<sup>44</sup>, and climate models<sup>28</sup>. However, most previous research focused on semi-direct effects of shallow clouds in the context of radiative forcing<sup>43</sup>, not precipitation. Hence, the overall uncertainty remains large.

Semi-direct effects of absorbing aerosol on the thermodynamic structure of the atmosphere are based on a sound physical foundation and have been well documented. However, the sign and magnitude of the effect on clouds and subsequently precipitation are sensitive to the vertical collocation of clouds and aerosols as well as the cloud regime. Some consistency exists across CRM studies; however, the

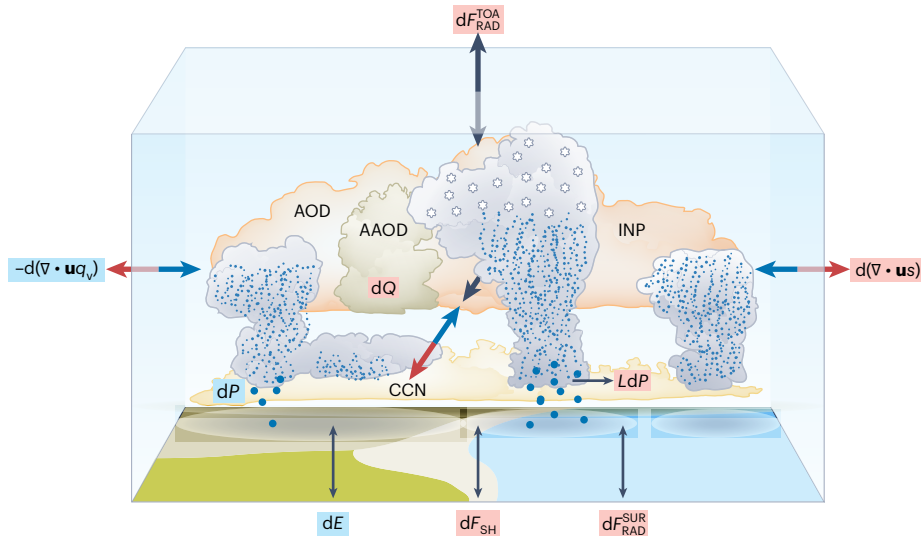


**Fig. 2 | Physical mechanisms of aerosols effects on precipitation.** Mechanisms of aerosol effects on precipitation and their constraints from an energy (red) and water (blue) budget perspective. Radiative and microphysical effects are mediated by variations in aerosol optical depth (AOD), aerosol absorption optical depth (AAOD) and cloud condensation nuclei (CCN) as well as ice nucleating particles (INP). RAD, radiative; SH, surface heat; SUR, surface; TOA, top of atmosphere.

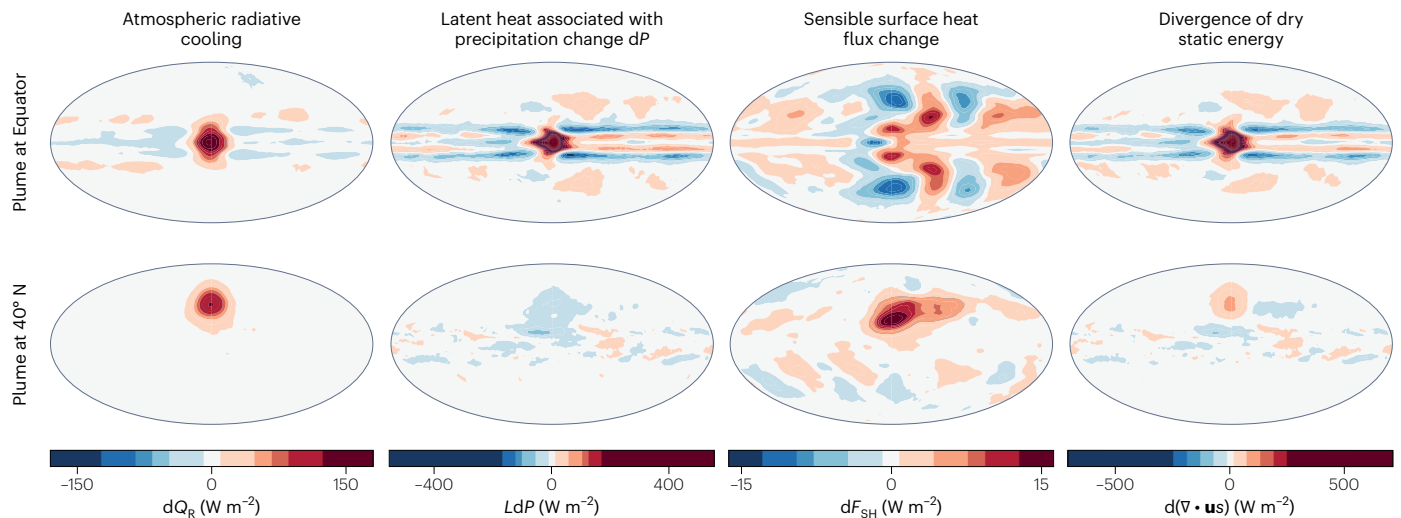


**Fig. 3 | Precipitation changes to idealized absorbing aerosol perturbations.** Idealized aqua-planet icosahedral non-hydrostatic (ICON)<sup>204</sup> general circulation model simulations of changes of precipitation and the atmospheric energy balance in response to idealized circular absorbing aerosol radiative plumes (of 10° size and identical aerosol radiative properties with peak aerosol optical depth of 2.4 and single scattering albedo of 0.8)<sup>33</sup>. Top row: plume located on the Equator. Bottom row: plume located at 40° N.  $dQ_R$ , atmospheric radiative cooling;  $LdP$ , latent heat associated with precipitation change  $dP$ ;  $dF_{SH}$ , sensible surface heat flux;  $d(\nabla \cdot us)$ , divergence of dry static energy.

observational evidence remains limited. We therefore assess this effect as category B, backed by physical conceptual models, modelling studies and limited observational evidence and some scientific consensus, even if the magnitude and sign of the impact on precipitation remain unclear.

The following three mechanisms could be combined as aerosol effects on regional precipitation patterns, but we retain the mechanistic separation prevailing in existing literature.

### Regional-scale and monsoon dynamics

Changes in regional-scale precipitation and monsoon dynamics have been attributed to regional patterns in ARI-induced surface cooling and atmospheric heating, both locally and remotely<sup>12,34,45–49</sup>. The precipitation response can be attributed to a combination of the modulation of surface fluxes over land, hence of the thermal gradient between land

and sea<sup>50,51</sup>, as well as aerosol absorption effects, driving thermally direct circulations<sup>12,52</sup> and moisture convergence<sup>52</sup> (linked to extreme precipitation<sup>53,54</sup>), the sea breeze circulation<sup>55</sup> and teleconnections<sup>56</sup>.

Aerosol effects on regional-scale precipitation and monsoon dynamics have been shown to affect precipitation patterns. This builds on climate model and CRM simulations and general physical understanding, with some observational evidence. However, uncertainties remain regarding the attribution of observed precipitation to aerosol effects and overall strength of the effects. We therefore assess this effect as category B, backed by some evidence and limited scientific consensus.

### Sea surface temperature patterns

Aerosol radiative effects on sea surface temperature (SST) patterns have been linked to observed climatological trends<sup>57,58</sup>. Associated

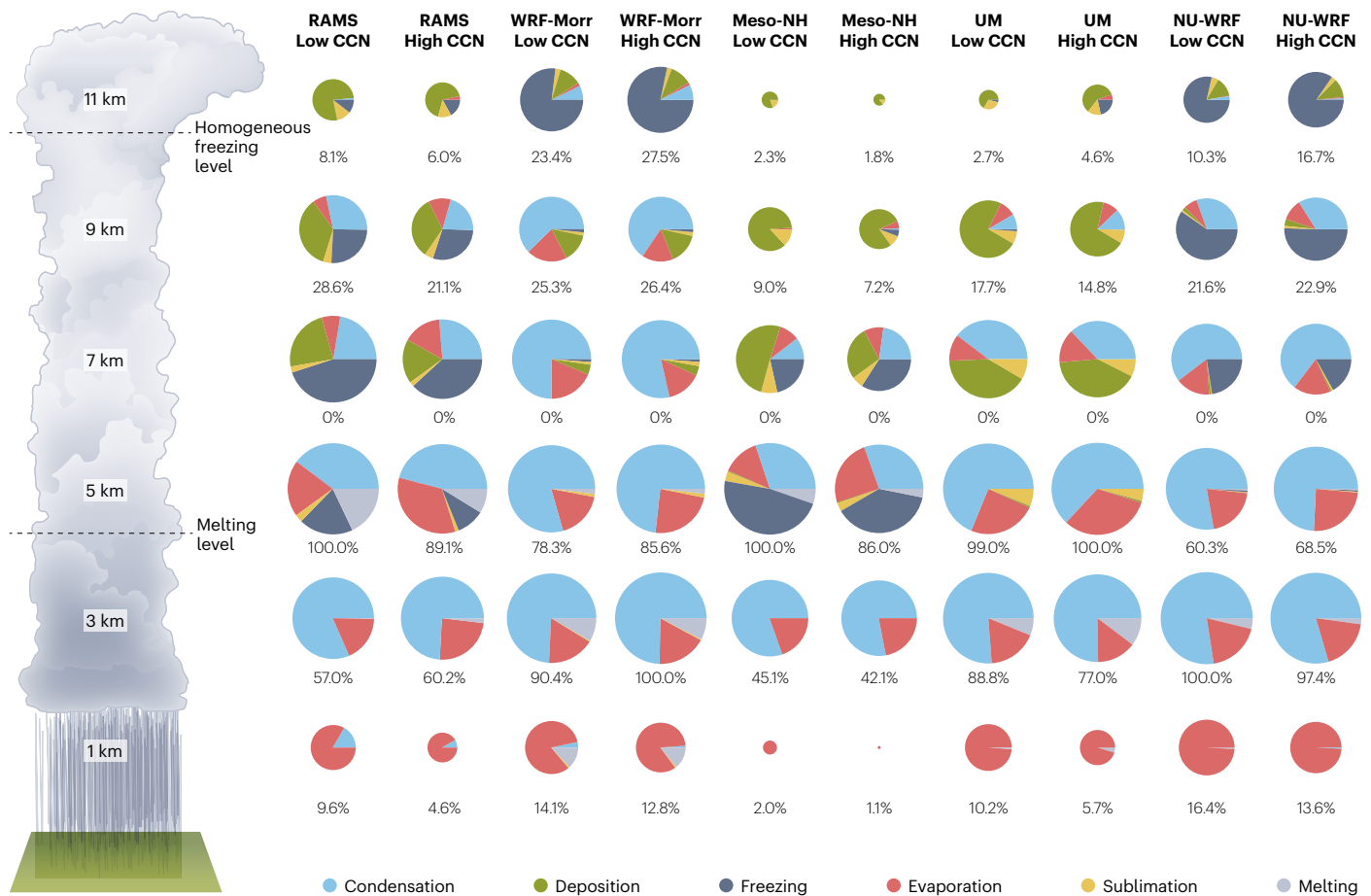


**Fig. 4 | Simulated aerosol effects on deep convection.** Cloud-resolving model intercomparison of CCN-mediated effects on deep convection from the Aerosol, Cloud, Precipitation and Climate deep convection study<sup>153</sup>; fractional mass process rates (%) for tracked deep convective systems for low- and high-CCN conditions as a function of height. Results for each model, named in the top row,

are shown for low- and high-CCN conditions in individual columns. The sizes of the pies are scaled logarithmically by the largest mass production rate of the model. Substantial differences in the model base state and the response to cloud condensation nuclei perturbations illustrate associated large uncertainties.

changes in multi-decadal SST variability<sup>59</sup> have previously been linked to the Sahel drought<sup>60–63</sup>. In addition to the local effects on the SST distribution, aerosols may affect ocean dynamics and thereby SSTs. For example, aerosol forcing was shown to strengthen the Atlantic meridional overturning circulation, thereby modulating SST patterns in the Atlantic Ocean<sup>64–67</sup> and affecting the Northern Hemisphere climate and precipitation patterns<sup>63,68</sup>. SSTs also control hurricane activity<sup>61,69–71</sup>, providing a mechanism for potential aerosol effects on hurricanes<sup>72,73</sup>. Forcing trends associated with European sulfur emissions as aerosol precursor have been linked to a pronounced North Atlantic ‘hurricane drought’ from the 1960s to the early 1990s<sup>74</sup>, during which hurricane power dissipation, a measure of storm damage<sup>75</sup>, was strongly inversely correlated with European sulfur emissions. Much of the direct SST forcing was from Saharan mineral dust, which in turn was associated with reduced monsoonal flow resulting from high sulfate aerosol concentrations<sup>76</sup>.

The SST-mediated effect of aerosol on regional precipitation patterns and hurricane activity builds on climate model simulations and general physical understanding, with limited observational evidence. We therefore assess this effect as category B, backed up by some evidence and limited scientific consensus.

### Hemispheric asymmetry

Hemispheric asymmetry in aerosol radiative effects<sup>77</sup> shifts the energy flux equator to where the column-integrated meridional energy flux vanishes<sup>78,79</sup>. The position of the energy flux equator is closely linked to

the intertropical convergence zone (ITCZ) position and associated precipitation. With anthropogenic aerosol located predominantly in the Northern Hemisphere, associated negative/positive aerosol radiative effects (for example, from sulfate/black carbon) lead to a southward/norward ITCZ shift<sup>62,78–87</sup>. For sulfate, this is a slow (SST-mediated) response, whereas for black carbon atmospheric adjustments to absorption contribute the response<sup>88</sup>. Dynamical cloud feedbacks can further amplify the hemispheric asymmetry<sup>89</sup>, and ITCZ shifts can interact with local monsoon regimes<sup>90</sup>.

The effect of hemispherically asymmetric aerosol radiative effects on the energy flux equator and ITCZ position builds on a robust theoretical foundation<sup>79</sup>, agrees with observational evidence<sup>83,91</sup> and is reliably reproduced by global climate models (GCMs). We therefore assess this effect as category A, backed by strong evidence and broad scientific consensus.

### Microphysical effects

#### CCN-mediated effects on stratiform liquid clouds

Cloud condensation nuclei (CCN) mediate effects on stratiform liquid clouds, including stratocumulus. Enhanced loading of CCN (hygroscopic or wettable aerosols of sufficient size to facilitate droplet growth) can increase cloud droplet numbers and, at constant liquid water content, lead to smaller droplets. This effect saturates for high aerosol concentrations<sup>92</sup> and/or low updraft velocities due to the depletion of supersaturation by condensation. This pathway can slow droplet growth to the threshold size for precipitation<sup>93–96</sup>, thereby suppressing

precipitation efficiency; this mechanism can also apply to the warm phase of stratiform mixed-phase clouds<sup>97</sup>. The reduced removal of cloud water by precipitation has been hypothesized to increase cloud liquid water path and lifetime<sup>95</sup>. There is clear observational evidence of an increase in cloud droplet numbers and associated decrease in droplet radii due to aerosol perturbations from aircraft data<sup>98</sup>, ship-track observations<sup>99–103</sup> and satellite remote sensing<sup>104–106</sup>. This is reproduced in CRMs and qualitatively in climate models<sup>105,107</sup>. Analysis of satellite-retrieved CloudSat<sup>108</sup> radar reflectivity and Moderate Resolution Imaging Spectroradiometer<sup>109</sup> effective radius data provides observational evidence for droplet size dependence of precipitation onset, with enhanced (low) drizzle rates above effective radii of 15 (10)  $\mu\text{m}$ . Combined with the documented impact of CCN on effective radii, this indicates warm-rain susceptibility to CCN perturbations<sup>110</sup>. These observations are limited to liquid-top shallow clouds, which represent a small fraction of global mean precipitation<sup>111</sup>. The observational evidence for an increase in liquid water paths via precipitation suppression due to increased aerosol concentrations is still disputed and cloud-regime dependent<sup>101,112–114</sup>. Many climate models simulate strong liquid water path responses to aerosol perturbations<sup>112,115</sup>, probably because their simplified representations of warm-rain formation ('autoconversion') have built-in power-law dependences on cloud droplet number but lack small-scale feedbacks, such as droplet size effects on evaporation and associated cloud entrainment feedbacks<sup>16,116,117</sup>. This uncertainty propagates into climate model assessments of APes.

CCN-mediated effects on stratiform liquid clouds, including stratocumulus, have been shown to increase droplet numbers and suppress warm-rain formation. This is consistent with warm-rain formation theory, supported by observational evidence from space-born cloud radars and reproduced by high-resolution CRMs. The expected effect is reduced light-rain occurrence, possibly compensated by increasing occurrence of stronger rain events. However, the overall impact on large-scale precipitation remains unclear. We therefore assess this effect as category B, backed by some evidence and limited scientific consensus.

The following two mechanisms could be combined as aerosol effects on convection, but we retain the mechanistic separation by cloud phase prevailing in existing literature.

### CCN-mediated effects on shallow convection

For shallow (liquid) convective clouds, an aerosol-mediated increase in cloud droplet numbers has several effects: associated smaller droplet radii enhance evaporation that increases the buoyancy gradient from cloud edge to centre, creating vorticity and increasing associated entrainment/detrainment<sup>116</sup>, which results in a reduction of cloud size, liquid water path, buoyancy and precipitation. At the same time, suppression of rain production via the droplet number effect on autoconversion can produce enhanced condensation and latent heat release due to larger numbers of cloud droplets and associated increase in surface area, often referred to as 'warm phase or condensational invigoration'<sup>118–120</sup>. It can also enhance cloud-top detrainment; subsequent evaporative cooling can destabilize the environment<sup>121</sup>. Both mechanisms could generate deeper clouds<sup>122</sup> with potentially enhanced precipitation. The net effect on mean precipitation could therefore be small<sup>16,17</sup> or even positive, depending on environmental conditions: high-resolution large-eddy simulations demonstrate a non-monotonic precipitation response with increases at low aerosol concentrations up to an optimal aerosol concentration, followed by a precipitation decrease<sup>118–120,123–125</sup>. For larger spatio-temporal scales, idealized simulations of shallow convection approach a radiative-convective equilibrium state<sup>17</sup>. Although the transient behaviour approaching equilibrium responds to increasing cloud droplet number concentrations through deepening and delayed precipitation onset<sup>126</sup>, in the equilibrium state, associated decreases in relative humidity and faster evaporation of small clouds compensate for much of the

effects with broader precipitation intensity distributions<sup>19</sup>. The overall effect depends on the relative importance of transient and equilibrium states<sup>17,93,127</sup>, with recent evidence highlighting limitations of idealized simulations that unrealistically favour equilibrium states<sup>128</sup>. However, contrasting environmental factors, such as boundary layer development or humidity, can influence the overall effects<sup>123,129</sup>.

CCN-mediated effects on shallow convection have been shown to increase droplet numbers and slow warm-phase precipitation formation. This is based on high-resolution CRMs and observational evidence. It is important to note that convection parameterizations in most GCMs do not represent any microphysical aerosol effects on convection. The overall effect on precipitation is less certain. We assess this effect as category B, backed by some evidence and limited scientific consensus.

### CCN-mediated effects on deep convection

For deep (liquid and ice phase) convective clouds, 'convective invigoration' is widely discussed, generally referring to enhanced aerosol levels causing stronger updrafts or higher clouds and an associated increase in precipitation<sup>93,98,130–136</sup>. Several hypotheses about underlying mechanisms exist. Often overlooked, these share a common starting point with shallow convection in the liquid base of clouds: the suppression of warm-rain formation from reduced autoconversion with enhanced CCN in the lower, liquid part of the cloud<sup>137</sup>, with an associated reduction in droplet size and resulting entrainment/detrainment feedbacks. Subsequent invigoration hypotheses include enhanced condensation and associated latent heat release (warm-phase invigoration; compare CCN-mediated effects on shallow convection)<sup>118,119,138,139</sup>; enhanced evaporation and downdraft formation affecting cold-pool strength and surface convergence<sup>140,141</sup>; delay of warm-phase precipitation increasing the amount of cloud water reaching the freezing level, enhancing the release of latent heat of freezing<sup>93,98,132</sup>, although the importance of this ('cold-phase invigoration') is disputed<sup>142</sup>; that depletion of cloud water through precipitation in low-aerosol environments could generate high supersaturations and subsequent activation of small aerosol particles into cloud droplets, enhancing condensation and (warm phase) latent heat release<sup>143</sup> (a hypothesis shown to be inconsistent with a limited set of observations)<sup>144</sup>; and that enhanced CCN levels increase environmental humidity through clouds mixing more condensed water into the surrounding air, preconditioning the environment for invigorated convection<sup>145</sup>. The last hypothesis is probably a consequence of idealized equilibrium simulations as it is not observed in realistic simulations across a wide range of environmental conditions<sup>146</sup>. Feedbacks between convective clouds and their thermodynamic environment may modulate or buffer APes. Overall, the strength and relative importance of mechanisms underlying convective invigoration are disputed<sup>142</sup>—it is sensitive to uncertain microphysical effects<sup>147,148</sup> and strongly dependent on environmental regimes<sup>49,130,140,149–151</sup>. In addition, the excess buoyancy associated with the respective mechanisms can be partially offset by negative buoyancy associated with condensate loading<sup>152,153</sup>, with the net effect dependent on condensate offloading through precipitation. The role of condensate loading has been explored through theoretical calculations that show the potential of aerosol-induced invigoration is limited for cold-based storms and that aerosol-induced cold-phase processes weaken, rather than strengthen, the updrafts in warm-based storms (referred to as aerosol enervation)<sup>154</sup>. The first systematic multimodel assessment of these competing aerosol effects on deep convective updrafts<sup>153</sup> has been performed as part of a deep convection case study<sup>153</sup> over Houston, Texas, USA, under the umbrella of the Aerosol, Cloud, Precipitation and Climate initiative (Fig. 4). This intercomparison revealed updraft increases by 5–15% in the mid-storm regions (4–7 km above ground) with increased CCN, driven primarily by enhanced condensation, with waning and mixed difference in levels above. Condensate loading contributions are generally limited. Despite this apparent invigoration, six of seven

models produce precipitation decreases (of 10–80%), highlighting the complexity of precipitation responses to aerosol perturbations. There are indications that microphysical effects strengthen deep and weaken shallow clouds in convective cloud fields, thereby broadening the precipitation intensity distribution<sup>18,44</sup>. Observations and modelling suggest a non-monotonic effect, with precipitation peaking at an optimal aerosol concentration<sup>155,156</sup>. It should be reiterated that even high-resolution CRM simulations of aerosol effects on deep convection remain subject to large uncertainty, particularly with mixed-phase and ice-cloud microphysics, affecting the simulated base states as well as their response to aerosol perturbations<sup>147</sup> (Fig. 4). Few current climate models include aerosol-aware convection parameterizations, and their early results indicate limited aerosol effects on convective precipitation on the global scale<sup>157,158</sup>. However, the associated uncertainties remain large, providing challenges for the next generation of cloud-resolving climate models.

CCN-mediated effects on deep convection consistently show increased droplet numbers and reduced warm-rain formation in the lower parts of the cloud. This builds on a robust theoretical foundation, is supported by limited observations and is consistently reproduced by CRMs. The propagation of these perturbations through the mixed- and ice-phase microphysics of clouds remains uncertain across models, with limited observational constraints. Several hypotheses exist on associated changes in buoyancies leading to invigoration, with models consistently simulating an increase in latent heating of condensation due to the increased surface area of enhanced droplet numbers. However, their importance remains highly uncertain. The overall effect on aggregated precipitation remains highly uncertain. We therefore assess this effect as category C, backed by plausible hypotheses but with limited evidence and limited scientific consensus.

### INP-mediated effects

Ice-nucleating particle (INP) effects on clouds are likely to be substantial, but still highly uncertain, given the unknown proportion of cloud ice between –38 and 0 °C that forms by INP-induced heterogeneous freezing or remains supercooled. Clouds glaciate below approximately –38 °C, where droplets freeze homogeneously. Increased concentrations of INPs (generally solid or crystalline aerosols that provide a surface onto which water molecules are likely to adsorb, bond and form ice-like aggregates) have been proposed to enhance the glaciation of clouds<sup>97,159,160</sup>, with an associated increase in precipitation efficiency and reduction of cloud lifetime<sup>161</sup>. Low INP concentrations in remote marine environments consistently inhibit precipitation<sup>162</sup>. However, the complexity of microphysical pathways in mixed- and ice-phase clouds is substantial<sup>148</sup>, with potential compensating pathways buffering the response, leading to low precipitation susceptibility<sup>163</sup>. Modification of precipitation through controlled INP emissions (‘cloud seeding’) has been extensively attempted in the weather modification community, with demonstrated impact on cloud microphysical processes<sup>164</sup>; however, limited evidence exists for its effectiveness in terms of large-scale precipitation modulation<sup>165,166</sup>. The role of INPs is further complicated by secondary ice production processes that are ill constrained but can lead to rapid cloud glaciation<sup>167</sup>.

INP-mediated effects have been shown to affect cloud phase and microphysics. A number of hypotheses exist on subsequent effects on precipitation. However, there is no complete theoretical framework, and evidence from modelling and observations is limited. We therefore assess this effect as category C, backed by plausible hypotheses but only limited evidence and limited scientific consensus.

It is important to reiterate that occurrence and strength, and spatio-temporal extent, of radiative and microphysical APEs are modulated by environmental conditions<sup>49,141,149,168,169</sup> as well as energy/water budget constraints<sup>11,33,36</sup>, which complicates their detectability. In addition, the potential exists for compensation between individual mechanisms, buffering the overall precipitation response<sup>16</sup>.

## Detectability and attribution of precipitation changes

In situ observations provide the most detailed insights into processes underlying APEs and are invaluable for the development and evaluation of theories and models. However, due to the inhomogeneous and intermittent nature of precipitation, it is generally impossible to measure areal average precipitation reliably. Representation errors<sup>170</sup> are likely to exceed the expected magnitude of aerosol effects.

Statistical analysis of satellite-retrieved aerosol radiative properties and precipitation shows higher precipitation rates with higher aerosol optical depth<sup>134</sup> with potentially non-monotonic behaviour<sup>171</sup>. Confounding factors (as aerosol extinction, cloud and precipitation are controlled by common factors, such as relative humidity<sup>172</sup>, and precipitation is the predominant aerosol sink<sup>173</sup>) complicate the interpretation. More fundamentally, remotely sensed aerosol properties are not always representative of the relevant aerosol perturbations<sup>174</sup>, and statistical analyses rely on assumptions of spatial representativeness of not co-located retrievals<sup>175,176</sup>. However, satellites provide the only source for global observational constraints, and the abundance of data permits robust statistical relationships. When environmental conditions are controlled for<sup>177</sup>, the apparent increase in precipitation with aerosol extinction is substantially reduced, although a positive relationship remains for cloud regimes<sup>177–179</sup> with tops colder than 0 °C, suggesting a role of ice processes<sup>178</sup>. Furthermore, satellite data provide constraints on microphysical processes: TRMM and CloudSat observations show a systematic shift in the relationship between raindrop size distribution and liquid water path with enhanced aerosol concentrations off the coast of Asia<sup>180</sup>.

Situations with well-characterised aerosol perturbations can serve as analogues for APEs<sup>181</sup>. Aerosols emitted from point sources, such as ships, volcanoes, industrial sites or cities, can cause distinct tracks in clouds that can be analysed from satellite data<sup>101,182,183</sup>, even when invisible<sup>184</sup>. The analysis of cloud droplet size in ship-track data shows a consistent effective radius reduction in the track<sup>99,113</sup>, consistent with observed effective radii reductions in response to SO<sub>2</sub> emissions from a degassing volcano<sup>112</sup>. In general, cloud droplet effective radius is expected to be positively correlated with precipitation formation through warm-rain formation<sup>185</sup>. However, the precipitation in ship tracks reveals a differentiated response across cloud regimes<sup>113</sup>. Satellite observations of lightning enhancement over shipping lanes<sup>186</sup> also provide strong indications of aerosol effects on convective microphysics and potential aerosol-driven mesoscale circulations, although APEs themselves remain more elusive<sup>187</sup>, and contributions from dynamical factors cannot be ruled out.

The difficulty remains to consistently reconcile observations with modelling data: any shift in the precipitation intensity distribution also implies a shift in the fraction of rain detectable from radar or microwave data<sup>188</sup>. In addition, the formation of detectable perturbations in clouds is limited to a subset of environmental conditions<sup>102,184</sup> with overall limited precipitation amounts, thereby limiting the global representativeness of such observations.

On larger scales, observational uncertainty and low signal-to-noise ratios complicate the attribution of observed changes of regional APEs<sup>189</sup>. Detection and attribution techniques<sup>190</sup> use GCMs to estimate spatio-temporal response patterns (‘fingerprints’) of precipitation to aerosol perturbations, which then can be compared with observed precipitation changes. However, observational and modelling uncertainties still obscure unambiguous evidence of such fingerprints of aerosol on regional-scale precipitation<sup>191–193</sup>.

## Overall assessment and new frontiers

This article reviews the evidence and scientific consensus for APEs and the underlying set of physical mechanisms. Broad consensus and strong theoretical evidence indicate that because global mean precipitation is constrained by conservation of energy<sup>6</sup> and water<sup>11,13</sup> as

well as surface evaporation<sup>25</sup>, aerosol radiative effects act as direct drivers of precipitation changes<sup>8</sup>. Likewise, aerosol radiative effects cause well-documented shifts of large-scale precipitation patterns, such as the ITCZ. The extent to which APEs are (1) applicable to smaller scales and (2) driven or buffered by compensating microphysical and dynamical mechanisms and budgetary constraints is less clear. Despite broad consensus and strong evidence that suitable aerosols increase cloud droplet numbers and reduce warm-rain formation efficiencies across cloud regimes, the overall aerosol effect on cloud microphysics and dynamics, as well as the subsequent impact on local, regional and global precipitation, is less constrained. Air-pollution control measures will reduce aerosol levels in the future, with an expected reversal of aerosol effects on regional precipitation patterns<sup>194</sup>.

Research on APEs has been limited by the fact that, locally to regionally, precipitation is controlled by complex nonlinear interactions with multiple microphysical, radiative and dynamical feedbacks; the expected aerosol-induced change in precipitation is potentially smaller than the internal variability<sup>195</sup> and uncertainty in current observations; current observations can constrain only some of the processes involved (satellite retrievals are often limited to proxies of the parameters involved and in situ measurements are limited, in particular in convective updrafts); isolating causal effects of aerosol on precipitation in the presence of multiple confounding variables remains challenging (it is easier to identify a strong ‘effect’ than to prove that it is the consequence of confounding); and finally, the representation of clouds in current climate models is inadequate to represent key microphysical processes and, importantly, the coupling between microphysics and cloud dynamics. Consequently, substantial uncertainty remains, limiting our ability to quantify and predict past and future precipitation changes.

We emphasize that, in terms of local impacts on humans and ecosystems, absolute precipitation changes are likely to be less important than relative precipitation changes in the mean and the frequency of occurrence of extremes. To illustrate this point, the absolute precipitation changes over the Sahel region simulated by the Coupled Model Intercomparison Project Phase 6 multimodel intercomparison seem negligible but constitute ~40% of the local precipitation (Fig. 1). Likewise, local impacts may be dominated by regional shifts of precipitation patterns rather than precipitation process changes. These aspects have not been given sufficient attention.

Out of ten mechanisms reviewed, only three have been assessed to be supported by strong evidence and broad consensus, and two are based primarily on hypotheses without consensus (Table 1). Future research should define critical tests for numerical models based on observations, in particular of convective updraft microphysics and thermodynamics, including observational simulators for comparability. Active remote sensing and systematic in situ observations<sup>196,197,198</sup>, including from uncrewed aerial vehicles, will provide novel constraints on particularly uncertain mixed-phase cloud microphysics and dynamics. Advanced geostationary satellites and cube-sat fleets will allow monitoring of the full cloud life cycle. Idealized aqua-planet<sup>33,199</sup> or radiative–convective equilibrium simulations<sup>18,200</sup>, such as the GAP Radiative Convective Equilibrium aerosol perturbation model intercomparison<sup>4</sup>, connect evidence from local-scale effects to regional and global precipitation. The availability of global CRMs<sup>201</sup> and digital twin Earths<sup>202</sup> provides important opportunities to overcome our reliance on climate models with parameterized local-scale processes and inadequate microphysics, which currently do not represent three of the ten mechanisms reviewed here (Table 1). However, even CRMs have large uncertainties in cloud microphysical processes that can obscure aerosol effects<sup>147</sup> and remain to be systematically constrained by observations. The shift to global CRMs, which will be a focus of the GAP initiative<sup>4</sup>, will also allow for robust quantification of the connection between local ACIs and large-scale dynamical feedbacks and teleconnections.

## References

1. IPCC: Summary for Policymakers. In *Climate Change 2014: Impacts, Adaptation, and Vulnerability. Part A: Global and Sectoral Aspects* (eds Field, C. B. et al.) (Cambridge Univ. Press, 2014).
2. Douville, H. et al. In *Climate Change 2021: The Physical Science Basis* (eds Masson-Delmotte, V. et al.) Ch. 8 (Cambridge Univ. Press, 2021).
3. Hartmann, D. L. et al. In *Climate Change 2013: The Physical Science Basis* (eds Stocker, T. F. et al.) Ch. 2 (Cambridge Univ. Press, 2013).
4. Stier, P., van den Heever, S. C. & Dagan, G. *The GEWEX Aerosol Precipitation Initiative* (GEWEX, 2023); <https://www.gewex.org/GAP/>
5. Mitchell, J. F. B., Wilson, C. A. & Cunningham, W. M. On CO<sub>2</sub> climate sensitivity and model dependence of results. *Q. J. R. Meteorol. Soc.* **113**, 293–322 (1987).
6. Allen, M. R. & Ingram, W. J. Constraints on future changes in climate and the hydrologic cycle. *Nature* **419**, 224–232 (2002).
7. Stephens, G. L. & Hu, Y. X. Are climate-related changes to the character of global-mean precipitation predictable? *Environ. Res. Lett.* **5**, 025209 (2010).
8. Muller, C. J. & O’Gorman, P. A. An energetic perspective on the regional response of precipitation to climate change. *Nat. Clim. Change* **1**, 266–271 (2011).
9. Myhre, G. et al. PDRMIP A Precipitation Driver and Response Model Intercomparison Project—protocol and preliminary results. *Bull. Am. Meteorol. Soc.* **98**, 1185–1198 (2017).
10. Richardson, T. B. et al. Drivers of precipitation change: an energetic understanding. *J. Clim.* **31**, 9641–9657 (2018).
11. Dagan, G. & Stier, P. Constraint on precipitation response to climate change by combination of atmospheric energy and water budgets. *NPJ Clim. Atmos. Sci.* **3**, 34 (2020).
12. Roeckner, E. et al. Impact of carbonaceous aerosol forcing on regional climate change. *Clim. Dyn.* **27**, 553–571 (2006).
13. Dagan, G., Stier, P. & Watson-Parris, D. Analysis of the atmospheric water budget for elucidating the spatial scale of precipitation changes under climate change. *Geophys. Res. Lett.* **46**, 10504–10511 (2019).
14. Trenberth, K. E., Dai, A., Rasmussen, R. M. & Parsons, D. B. The changing character of precipitation. *Bull. Am. Meteorol. Soc.* **84**, 1205–1218 (2003).
15. Hodnebrog, Ø. et al. Water vapour adjustments and responses differ between climate drivers. *Atmos. Chem. Phys.* **19**, 12887–12899 (2019).
16. Stevens, B. & Feingold, G. Untangling aerosol effects on clouds and precipitation in a buffered system. *Nature* **461**, 607–613 (2009).
17. Seifert, A., Heus, T., Pincus, R. & Stevens, B. Large-eddy simulation of the transient and near-equilibrium behavior of precipitating shallow convection. *J. Adv. Model. Earth Syst.* **7**, 1918–1937 (2015).
18. van den Heever, S. C., Stephens, G. L. & Wood, N. B. Aerosol indirect effects on tropical convection characteristics under conditions of radiative–convective equilibrium. *J. Atmos. Sci.* **68**, 699–718 (2011).
19. Yamaguchi, T., Feingold, G. & Kazil, J. Aerosol–cloud interactions in trade wind cumulus clouds and the role of vertical wind shear. *J. Geophys. Res. Atmos.* **124**, 12244–12261 (2019).
20. Richardson, T. B., Samset, B. H., Andrews, T., Myhre, G. & Forster, P. M. An assessment of precipitation adjustment and feedback computation methods. *J. Geophys. Res. Atmos.* **121**, 11608–11619 (2016).
21. Samset, B. H. et al. Fast and slow precipitation responses to individual climate forcings: A PDRMIP multimodel study. *Geophys. Res. Lett.* **43**, 2782–2791 (2016).
22. Flaschner, D., Mauritsen, T. & Stevens, B. Understanding the intermodel spread in global-mean hydrological sensitivity. *J. Clim.* **29**, 801–817 (2016).



23. Dagan, G., Yeheskel, N. & Williams, A. I. L. Radiative forcing from aerosol-cloud interactions enhanced by large-scale circulation adjustments. *Nat. Geosci.* **16**, 1092–1098 (2023).
24. Williams, A. I. L., Watson-Parris, D., Dagan, G. & Stier, P. Dependence of fast changes in global and local precipitation on the geographical location of absorbing aerosol. *J. Clim.* **36**, 6163–6176 (2023).
25. Ramanathan, V., Crutzen, P. J., Kiehl, J. T. & Rosenfeld, D. Atmosphere—aerosols, climate, and the hydrological cycle. *Science* **294**, 2119–2124 (2001).
26. Trenberth, K. E. & Dai, A. Effects of Mount Pinatubo volcanic eruption on the hydrological cycle as an analog of geoengineering. *Geophys. Res. Lett.* <https://doi.org/10.1029/2007GL030524> (2007).
27. Oman, L., Robock, A., Stenchikov, G. L. & Thordarson, T. High-latitude eruptions cast shadow over the African monsoon and the flow of the Nile. *Geophys. Res. Lett.* <https://doi.org/10.1029/2006gl027665> (2006).
28. Ming, Y., Ramaswamy, V. & Persad, G. Two opposing effects of absorbing aerosols on global-mean precipitation. *Geophys. Res. Lett.* <https://doi.org/10.1029/2010gl042895> (2010).
29. Boucher, O. et al. In *Climate Change 2013: The Physical Science Basis* (eds Fuzzi, S. et al.) Ch. 7 (Cambridge Univ. Press, 2013).
30. Myhre, G. et al. Sensible heat has significantly affected the global hydrological cycle over the historical period. *Nat. Commun.* **9**, 1922 (2018).
31. Salzmann, M. Global warming without global mean precipitation increase? *Sci. Adv.* **2**, e1501572 (2016).
32. Wu, P., Christidis, N. & Stott, P. Anthropogenic impact on Earth's hydrological cycle. *Nat. Clim. Change* **3**, 807–810 (2013).
33. Dagan, G., Stier, P. & Watson-Parris, D. Contrasting response of precipitation to aerosol perturbation in the tropics and extratropics explained by energy budget considerations. *Geophys. Res. Lett.* **46**, 7828–7837 (2019).
34. Hodnebrog, O., Myhre, G., Forster, P. M., Sillmann, J. & Samset, B. H. Local biomass burning is a dominant cause of the observed precipitation reduction in southern Africa. *Nat. Commun.* **7**, 11236 (2016).
35. O’Gorman, P. A., Allan, R. P., Byrne, M. P. & Previdi, M. Energetic constraints on precipitation under climate change. *Surv. Geophys.* **33**, 585–608 (2012).
36. Dagan, G., Stier, P. & Watson-Parris, D. An energetic view on the geographical dependence of the fast aerosol radiative effects on precipitation. *J. Geophys. Res. Atmos.* **126**, e2020JD033045 (2021).
37. Jiang, H. L. & Feingold, G. Effect of aerosol on warm convective clouds: aerosol–cloud–surface flux feedbacks in a new coupled large eddy model. *J. Geophys. Res. Atmos.* <https://doi.org/10.1029/2005JD006138> (2006).
38. Hansen, J., Sato, M. & Ruedy, R. Radiative forcing and climate response. *J. Geophys. Res. Atmos.* **102**, 6831–6864 (1997).
39. Ackerman, A. S. et al. Reduction of tropical cloudiness by soot. *Science* **288**, 1042–1047 (2000).
40. Sand, M., Samset, B. H., Tsigaridis, K., Bauer, S. E. & Myhre, G. Black carbon and precipitation: an energetics perspective. *J. Geophys. Res. Atmos.* **125**, e2019JD032239 (2020).
41. Johnson, B. T., Shine, K. P. & Forster, P. M. The semi-direct aerosol effect: impact of absorbing aerosols on marine stratocumulus. *Q. J. R. Meteorol. Soc.* **130**, 1407–1422 (2004).
42. Yamaguchi, T., Feingold, G., Kazil, J. & McComiskey, A. Stratocumulus to cumulus transition in the presence of elevated smoke layers. *Geophys. Res. Lett.* **42**, 10478–10485 (2015).
43. Redemann, J. et al. An overview of the ORACLES (Observations of Aerosols above CLouds and their intERactionS) project: aerosol–cloud–radiation interactions in the southeast Atlantic basin. *Atmos. Chem. Phys.* **21**, 1507–1563 (2021).
44. Herbert, R., Stier, P. & Dagan, G. Isolating large-scale smoke impacts on cloud and precipitation processes over the Amazon with convection permitting resolution. *J. Geophys. Res. Atmos.* **126**, e2021JD034615 (2021).
45. Menon, S., Hansen, J., Nazarenko, L. & Luo, Y. F. Climate effects of black carbon aerosols in China and India. *Science* **297**, 2250–2253 (2002).
46. Bollasina, M. A., Ming, Y. & Ramaswamy, V. Anthropogenic aerosols and the weakening of the South Asian summer monsoon. *Science* **334**, 502–505 (2011).
47. Wang, C. A modeling study on the climate impacts of black carbon aerosols. *J. Geophys. Res. Atmos.* <https://doi.org/10.1029/2003jd004084> (2004).
48. Leung, G. R. & van den Heever, S. C. Aerosol breezes drive cloud and precipitation increases. *Nat. Commun.* **14**, 2508 (2023).
49. Fan, J. W. et al. Dominant role by vertical wind shear in regulating aerosol effects on deep convective clouds. *J. Geophys. Res. Atmos.* <https://doi.org/10.1029/2009jd012352> (2009).
50. Li, X. Q. et al. South Asian Summer Monsoon response to aerosol-forced sea surface temperatures. *Geophys. Res. Lett.* <https://doi.org/10.1029/2019GL085329> (2020).
51. Zanis, P. et al. Fast responses on pre-industrial climate from present-day aerosols in a CMIP6 multi-model study. *Atmos. Chem. Phys.* **20**, 8381–8404 (2020).
52. Wang, C., Kim, D., Ekman, A. M. L., Barth, M. C. & Rasch, P. J. Impact of anthropogenic aerosols on Indian summer monsoon. *Geophys. Res. Lett.* <https://doi.org/10.1029/2009gl040114> (2009).
53. O’Gorman, P. A. & Schneider, T. The physical basis for increases in precipitation extremes in simulations of 21st-century climate change. *Proc. Natl Acad. Sci. USA* **106**, 14773–14777 (2009).
54. Singh, D., Bollasina, M., Ting, M. F. & Diffenbaugh, N. S. Disentangling the influence of local and remote anthropogenic aerosols on South Asian monsoon daily rainfall characteristics. *Clim. Dyn.* **52**, 6301–6320 (2019).
55. Grant, L. D. & van den Heever, S. C. Aerosol–cloud–land surface interactions within tropical sea breeze convection. *J. Geophys. Res. Atmos.* **119**, 8340–8361 (2014).
56. Bollasina, M. A., Ming, Y., Ramaswamy, V., Schwarzkopf, M. D. & Naik, V. Contribution of local and remote anthropogenic aerosols to the twentieth century weakening of the South Asian monsoon. *Geophys. Res. Lett.* **41**, 680–687 (2014).
57. Booth, B. B. B., Dunstone, N. J., Halloran, P. R., Andrews, T. & Bellouin, N. Aerosols implicated as a prime driver of twentieth-century North Atlantic climate variability. *Nature* **484**, 228–232 (2012).
58. Undorf, S., Bollasina, M. A., Booth, B. B. B. & Hegerl, G. C. Contrasting the effects of the 1850–1975 increase in sulphate aerosols from North America and Europe on the Atlantic in the CESM. *Geophys. Res. Lett.* **45**, 11930–11940 (2018).
59. Wilcox, L. J., Highwood, E. J. & Dunstone, N. J. The influence of anthropogenic aerosol on multi-decadal variations of historical global climate. *Environ. Res. Lett.* **8**, 024033 (2013).
60. Folland, C. K., Palmer, T. N. & Parker, D. E. Sahel rainfall and worldwide sea temperatures, 1901–85. *Nature* **320**, 602–607 (1986).
61. Zhang, R. & Delworth, T. L. Impact of Atlantic multidecadal oscillations on India/Sahel rainfall and Atlantic hurricanes. *Geophys. Res. Lett.* <https://doi.org/10.1029/2006gl026267> (2006).
62. Rotstayn, L. D. & Lohmann, U. Tropical rainfall trends and the indirect aerosol effect. *J. Clim.* **15**, 2103–2116 (2002).
63. Zhang, S., Stier, P., Dagan, G. & Wang, M. Anthropogenic aerosols modulated twentieth-century Sahel rainfall variability. *Geophys. Res. Lett.* <https://doi.org/10.1029/2021GL095629> (2021).
64. Menary, M. B. et al. Aerosol-forced AMOC changes in CMIP6 historical simulations. *Geophys. Res. Lett.* **47**, e2020GL088166 (2020).

65. Cai, W. et al. Pan-oceanic response to increasing anthropogenic aerosols: impacts on the Southern Hemisphere oceanic circulation. *Geophys. Res. Lett.* <https://doi.org/10.1029/2006gl027513> (2006).
66. Delworth, T. L. & Dixon, K. W. Have anthropogenic aerosols delayed a greenhouse gas-induced weakening of the North Atlantic thermohaline circulation? *Geophys. Res. Lett.* <https://doi.org/10.1029/2005gl024980> (2006).
67. Dagan, G., Stier, P. & Watson-Parris, D. Aerosol forcing masks and delays the formation of the North Atlantic warming hole by three decades. *Geophys. Res. Lett.* **47**, e2020GL090778 (2020).
68. Haarsma, R. J., Selten, F. M. & Drijfhout, S. S. Decelerating Atlantic meridional overturning circulation main cause of future west European summer atmospheric circulation changes. *Environ. Res. Lett.* **10**, 094007 (2015).
69. Goldenberg, S. B., Landsea, C. W., Mestas-Nunez, A. M. & Gray, W. M. The recent increase in Atlantic hurricane activity: causes and implications. *Science* **293**, 474–479 (2001).
70. Trenberth, K. Uncertainty in hurricanes and global warming. *Science* **308**, 1753–1754 (2005).
71. Emanuel, K. & Sobel, A. Response of tropical sea surface temperature, precipitation, and tropical cyclone-related variables to changes in global and local forcing. *J. Adv. Model. Earth Syst.* **5**, 447–458 (2013).
72. Chiacchio, M. et al. On the links between meteorological variables, aerosols, and tropical cyclone frequency in individual ocean basins. *J. Geophys. Res. Atmos.* **122**, 802–822 (2017).
73. Jones, A. C. et al. Impacts of hemispheric solar geoengineering on tropical cyclone frequency. *Nat. Commun.* **8**, 1382 (2017).
74. Mann, M. E. & Emanuel, K. A. Atlantic hurricane trends linked to climate change. *Eos* **87**, 233–241 (2011).
75. Emanuel, K. Increasing destructiveness of tropical cyclones over the past 30 years. *Nature* **436**, 686–688 (2005).
76. Rousseau-Rizzi, R. *On the Climate Variability of Tropical Cyclone Potential Intensity and Atlantic Hurricane Activity* (MIT, 2021).
77. Myhre, G. et al. Radiative forcing of the direct aerosol effect from AeroCom Phase II simulations. *Atmos. Chem. Phys.* **13**, 1853–1877 (2013).
78. Kang, S. M., Held, I. M., Frierson, D. M. W. & Zhao, M. The response of the ITCZ to extratropical thermal forcing: idealized slab–ocean experiments with a GCM. *J. Clim.* **21**, 3521–3532 (2008).
79. Adam, O., Bischoff, T. & Schneider, T. Seasonal and interannual variations of the energy flux equator and ITCZ. Part I: zonally averaged ITCZ position. *J. Clim.* **29**, 3219–3230 (2016).
80. Kristjansson, J. E., Iversen, T., Kirkevåg, A., Seland, O. & Debernard, J. Response of the climate system to aerosol direct and indirect forcing: role of cloud feedbacks. *J. Geophys. Res. Atmos.* <https://doi.org/10.1029/2005jd006299> (2005).
81. Broccoli, A. J., Dahl, K. A. & Stouffer, R. J. Response of the ITCZ to Northern Hemisphere cooling. *Geophys. Res. Lett.* <https://doi.org/10.1029/2005gl024546> (2006).
82. Wang, C. The sensitivity of tropical convective precipitation to the direct radiative forcings of black carbon aerosols emitted from major regions. *Ann. Geophys.* **27**, 3705–3711 (2009).
83. Haywood, J. M., Jones, A., Bellouin, N. & Stephenson, D. Asymmetric forcing from stratospheric aerosols impacts Sahelian rainfall. *Nat. Clim. Change* **3**, 660–665 (2013).
84. Navarro, J. C. A. et al. Future response of temperature and precipitation to reduced aerosol emissions as compared with increased greenhouse gas concentrations. *J. Clim.* **30**, 939–954 (2017).
85. Voigt, A. et al. Fast and slow shifts of the zonal-mean intertropical convergence zone in response to an idealized anthropogenic aerosol. *J. Adv. Model. Earth Syst.* **9**, 870–892 (2017).
86. Hawcroft, M., Haywood, J. M., Collins, M. & Jones, A. The contrasting climate response to tropical and extratropical energy perturbations. *Clim. Dyn.* **51**, 3231–3249 (2018).
87. Zhao, S. Y. & Suzuki, K. Differing impacts of black carbon and sulfate aerosols on global precipitation and the ITCZ location via atmosphere and ocean energy perturbations. *J. Clim.* **32**, 5567–5582 (2019).
88. Zhang, S. P., Stier, P. & Watson-Parris, D. On the contribution of fast and slow responses to precipitation changes caused by aerosol perturbations. *Atmos. Chem. Phys.* **21**, 10179–10197 (2021).
89. Soden, B. & Chung, E. S. The large-scale dynamical response of clouds to aerosol forcing. *J. Clim.* **30**, 8783–8794 (2017).
90. Hari, V., Villarini, G., Karmakar, S., Wilcox, L. J. & Collins, M. Northward propagation of the Intertropical Convergence Zone and strengthening of Indian summer monsoon rainfall. *Geophys. Res. Lett.* **47**, e2020GL089823 (2020).
91. Allen, R. J., Evan, A. T. & Booth, B. B. Interhemispheric aerosol radiative forcing and tropical precipitation shifts during the late twentieth century. *J. Clim.* **28**, 8219–8246 (2015).
92. Reutter, P. et al. Aerosol- and updraft-limited regimes of cloud droplet formation: influence of particle number, size and hygroscopicity on the activation of cloud condensation nuclei (CCN). *Atmos. Chem. Phys.* **9**, 7067–7080 (2009).
93. Williams, E. et al. Contrasting convective regimes over the Amazon: implications for cloud electrification. *J. Geophys. Res. Atmos.* <https://doi.org/10.1029/2001jd000380> (2002).
94. L’Ecuyer, T. S., Berg, W., Haynes, J., Lebsock, M. & Takemura, T. Global observations of aerosol impacts on precipitation occurrence in warm maritime clouds. *J. Geophys. Res. Atmos.* <https://doi.org/10.1029/2008jd011273> (2009).
95. Albrecht, B. A. Aerosols, cloud microphysics, and fractional cloudiness. *Science* **245**, 1227–1230 (1989).
96. Twomey, S. Pollution and the planetary albedo. *Atmos. Environ.* **8**, 1251–1256 (1974).
97. Possner, A., Ekman, A. M. L. & Lohmann, U. Cloud response and feedback processes in stratiform mixed-phase clouds perturbed by ship exhaust. *Geophys. Res. Lett.* **44**, 1964–1972 (2017).
98. Andreae, M. O. et al. Smoking rain clouds over the Amazon. *Science* **303**, 1337–1342 (2004).
99. Durkee, P. A. et al. The impact of ship-produced aerosols on the microstructure and albedo of warm marine stratocumulus clouds: a test of MAST hypotheses 1i and 1ii. *J. Atmos. Sci.* **57**, 2554–2569 (2000).
100. Christensen, M. W., Suzuki, K., Zambri, B. & Stephens, G. L. Ship track observations of a reduced shortwave aerosol indirect effect in mixed-phase clouds. *Geophys. Res. Lett.* **41**, 6970–6977 (2014).
101. Toll, V., Christensen, M., Gasso, S. & Bellouin, N. Volcano and ship tracks indicate excessive aerosol-induced cloud water increases in a climate model. *Geophys. Res. Lett.* **44**, 12492–12500 (2017).
102. Gryspeerdt, E., Smith, T. W. P., O’Keeffe, E., Christensen, M. W. & Goldsworth, F. W. The impact of ship emission controls recorded by cloud properties. *Geophys. Res. Lett.* **46**, 12547–12555 (2019).
103. Watson-Parris, D. et al. Shipping regulations lead to large reduction in cloud perturbations. *Proc. Natl Acad. Sci. USA* **119**, e2206885119 (2022).
104. Quaas, J., Boucher, O. & Lohmann, U. Constraining the total aerosol indirect effect in the LMDZ and ECHAM4 GCMs using MODIS satellite data. *Atmos. Chem. Phys.* **6**, 947–955 (2006).
105. Quaas, J. et al. Aerosol indirect effects—general circulation model intercomparison and evaluation with satellite data. *Atmos. Chem. Phys.* **9**, 8697–8717 (2009).
106. Rosenfeld, D. et al. Global observations of aerosol–cloud–precipitation–climate interactions. *Rev. Geophys.* **52**, 750–808 (2014).

107. Bellouin, N. et al. Bounding global aerosol radiative forcing of climate change. *Rev. Geophys.* **58**, e2019RG000660 (2020).
108. Stephens, G. et al. CloudSat and CALIPSO within the A-Train: ten years of actively observing the Earth system. *Bull. Am. Meteorol. Soc.* **99**, 569–581 (2018).
109. Platnick, S. et al. The MODIS cloud optical and microphysical products: Collection 6 updates and examples from Terra and Aqua. *IEEE Trans. Geosci. Remote Sens.* **55**, 502–525 (2017).
110. Suzuki, K., Nakajima, T. Y. & Stephens, G. L. Particle growth and drop collection efficiency of warm clouds as inferred from joint CloudSat and MODIS observations. *J. Atmos. Sci.* **67**, 3019–3032 (2010).
111. Mulmenstadt, J., Sourdeval, O., Delanoe, J. & Quaas, J. Frequency of occurrence of rain from liquid-, mixed-, and ice-phase clouds derived from A-Train satellite retrievals. *Geophys. Res. Lett.* **42**, 6502–6509 (2015).
112. Malavelle, F. F. et al. Strong constraints on aerosol–cloud interactions from volcanic eruptions. *Nature* **546**, 485–491 (2017).
113. Christensen, M. W. & Stephens, G. L. Microphysical and macrophysical responses of marine stratocumulus polluted by underlying ships: 2. Impacts of haze on precipitating clouds. *J. Geophys. Res. Atmos.* <https://doi.org/10.1029/2011JD017125> (2012).
114. McCoy, D. T. et al. Aerosol midlatitude cyclone indirect effects in observations and high-resolution simulations. *Atmos. Chem. Phys.* **18**, 5821–5846 (2018).
115. Gryspeerd, E. et al. Surprising similarities in model and observational aerosol radiative forcing estimates. *Atmos. Chem. Phys.* **20**, 613–623 (2020).
116. Jiang, H., Xue, H., Teller, A., Feingold, G. & Levin, Z. Aerosol effects on the lifetime of shallow cumulus. *Geophys. Res. Lett.* <https://doi.org/10.1029/2006GL026024> (2006).
117. Zhou, C. & Penner, J. E. Why do general circulation models overestimate the aerosol cloud lifetime effect? A case study comparing CAM5 and a CRM. *Atmos. Chem. Phys.* **17**, 21–29 (2017).
118. Koren, I., Dagan, G. & Altaratz, O. From aerosol-limited to invigoration of warm convective clouds. *Science* **344**, 1143–1146 (2014).
119. Seiki, T. & Nakajima, T. Aerosol effects of the condensation process on a convective cloud simulation. *J. Atmos. Sci.* **71**, 833–853 (2014).
120. Sheffield, A. M., Saleeby, S. M. & van den Heever, S. C. Aerosol-induced mechanisms for cumulus congestus growth. *J. Geophys. Res. Atmos.* **120**, 8941–8952 (2015).
121. Xue, H. & Feingold, G. Large-eddy simulations of trade wind cumuli: investigation of aerosol indirect effects. *J. Atmos. Sci.* **63**, 1605–1622 (2006).
122. Stevens, B. & Seifert, A. Understanding macrophysical outcomes of microphysical choices in simulations of shallow cumulus convection. *J. Meteorol. Soc. Jpn.* **2** **86A**, 143–162 (2008).
123. Dagan, G., Koren, I. & Altaratz, O. Aerosol effects on the timing of warm rain processes. *Geophys. Res. Lett.* **42**, 4590–4598 (2015).
124. Dagan, G., Koren, I. & Altaratz, O. Competition between core and periphery-based processes in warm convective clouds— from invigoration to suppression. *Atmos. Chem. Phys.* **15**, 2749–2760 (2015).
125. Kogan, Y. L. & Martin, W. J. Parameterization of bulk condensation in numerical cloud models. *J. Atmos. Sci.* **51**, 1728–1739 (1994).
126. Seifert, A. & Heus, T. Large-eddy simulation of organized precipitating trade wind cumulus clouds. *Atmos. Chem. Phys.* **13**, 5631–5645 (2013).
127. Dagan, G., Koren, I., Altaratz, O. & Lehahn, Y. Shallow convective cloud field lifetime as a key factor for evaluating aerosol effects. *iScience* **10**, 192–202 (2018).
128. Spill, G., Stier, P., Field, P. R. & Dagan, G. Effects of aerosol in simulations of realistic shallow cumulus cloud fields in a large domain. *Atmos. Chem. Phys.* **19**, 13507–13517 (2019).
129. Chen, Y. C., Christensen, M. W., Stephens, G. L. & Seinfeld, J. H. Satellite-based estimate of global aerosol–cloud radiative forcing by marine warm clouds. *Nat. Geosci.* **7**, 643–646 (2014).
130. Khain, A., Rosenfeld, D. & Pokrovsky, A. Aerosol impact on the dynamics and microphysics of deep convective clouds. *Q. J. R. Meteorol. Soc.* **131**, 2639–2663 (2005).
131. van den Heever, S. C., Carrio, G. G., Cotton, W. R., DeMott, P. J. & Prenni, A. J. Impacts of nucleating aerosol on Florida storms. Part I: mesoscale simulations. *J. Atmos. Sci.* **63**, 1752–1775 (2006).
132. Rosenfeld, D. et al. Flood or drought: how do aerosols affect precipitation? *Science* **321**, 1309–1313 (2008).
133. Tao, W. K., Chen, J. P., Li, Z. Q., Wang, C. & Zhang, C. D. Impact of aerosols on convective clouds and precipitation. *Rev. Geophys.* <https://doi.org/10.1029/2011rg000369> (2012).
134. Koren, I. et al. Aerosol-induced intensification of rain from the tropics to the mid-latitudes. *Nat. Geosci.* **5**, 118–122 (2012).
135. Koren, I., Kaufman, Y. J., Rosenfeld, D., Remer, L. A. & Rudich, Y. Aerosol invigoration and restructuring of Atlantic convective clouds. *Geophys. Res. Lett.* <https://doi.org/10.1029/2005GL023187> (2005).
136. Clavner, M., Cotton, W. R., van den Heever, S. C., Saleeby, S. M. & Pierce, J. R. The response of a simulated mesoscale convective system to increased aerosol pollution: part I: precipitation intensity, distribution, and efficiency. *Atmos. Res.* **199**, 193–208 (2018).
137. Storer, R. L. & Van den Heever, S. C. Microphysical processes evident in aerosol forcing of tropical deep convective clouds. *J. Atmos. Sci.* **70**, 430–446 (2013).
138. Wang, C. A modeling study of the response of tropical deep convection to the increase of cloud condensation nuclei concentration: 1. Dynamics and microphysics. *J. Geophys. Res. Atmos.* <https://doi.org/10.1029/2004jd005720> (2005).
139. Chua, X. R. & Ming, Y. Convective invigoration traced to warm-rain microphysics. *Geophys. Res. Lett.* <https://doi.org/10.1029/2020GL089134> (2020).
140. Lee, S. S., Donner, L. J., Phillips, V. T. J. & Ming, Y. Examination of aerosol effects on precipitation in deep convective clouds during the 1997 ARM summer experiment. *Q. J. R. Meteorol. Soc.* **134**, 1201–1220 (2008).
141. Grant, L. D. & van den Heever, S. C. Cold pool and precipitation responses to aerosol loading: modulation by dry layers. *J. Atmos. Sci.* **72**, 1398–1408 (2015).
142. Varble, A. C., Igel, A. L., Morrison, H., Grabowski, W. W. & Lebo, Z. J. Opinion: a critical evaluation of the evidence for aerosol invigoration of deep convection. *Atmos. Chem. Phys.* **23**, 13791–13808 (2023).
143. Fan, J. W. et al. Substantial convection and precipitation enhancements by ultrafine aerosol particles. *Science* **359**, 411–418 (2018).
144. Romps, D. M. et al. Air pollution unable to intensify storms via warm-phase invigoration. *Geophys. Res. Lett.* <https://doi.org/10.1029/2022gl100409> (2023).
145. Abbott, T. H. & Cronin, T. W. Aerosol invigoration of atmospheric convection through increases in humidity. *Science* **371**, 83–85 (2021).
146. Dagan, G. et al. Boundary conditions representation can determine simulated aerosol effects on convective cloud fields. *Commun. Earth Environ.* **3**, 71 (2022).
147. White, B. et al. Uncertainty from the choice of microphysics scheme in convection-permitting models significantly exceeds aerosol effects. *Atmos. Chem. Phys.* **17**, 12145–12175 (2017).

148. Heikenfeld, M., White, B., Labbouz, L. & Stier, P. Aerosol effects on deep convection: the propagation of aerosol perturbations through convective cloud microphysics. *Atmos. Chem. Phys.* **19**, 2601–2627 (2019).
149. Storer, R. L., van den Heever, S. C. & Stephens, G. L. Modeling aerosol impacts on convective storms in different environments. *J. Atmos. Sci.* **67**, 3904–3915 (2010).
150. Miltenberger, A. K. et al. Aerosol–cloud interactions in mixed-phase convective clouds—part 1: aerosol perturbations. *Atmos. Chem. Phys.* **18**, 3119–3145 (2018).
151. Lee, S. S., Donner, L. J. & Penner, J. E. Thunderstorm and stratocumulus: how does their contrasting morphology affect their interactions with aerosols? *Atmos. Chem. Phys.* **10**, 6819–6837 (2010).
152. Grabowski, W. W. Untangling microphysical impacts on deep convection applying a novel modeling methodology. *J. Atmos. Sci.* **72**, 2446–2464 (2015).
153. Marinescu, P. J. et al. Impacts of varying concentrations of cloud condensation nuclei on deep convective cloud updrafts—a multimodel assessment. *J. Atmos. Sci.* **78**, 1147–1172 (2021).
154. Igel, A. L. & van den Heever, S. C. Invigoration or enervation of convective clouds by aerosols? *Geophys. Res. Lett.* **48**, e2021GL093804 (2021).
155. Connolly, P. J. et al. Cloud-resolving simulations of intense tropical Hector thunderstorms: implications for aerosol–cloud interactions. *Q. J. R. Meteorol. Soc.* **132**, 3079–3106 (2006).
156. Pan, Z. X. et al. Observational quantification of aerosol invigoration for deep convective cloud lifecycle properties based on geostationary satellite. *J. Geophys. Res. Atmos.* <https://doi.org/10.1029/2020JD034275> (2021).
157. Kipling, Z., Labbouz, L. & Stier, P. Global response of parameterised convective cloud fields to anthropogenic aerosol forcing. *Atmos. Chem. Phys.* **20**, 4445–4460 (2020).
158. Lohmann, U. Global anthropogenic aerosol effects on convective clouds in ECHAM5-HAM. *Atmos. Chem. Phys.* **8**, 2115–2131 (2008).
159. Choi, Y. S., Lindzen, R. S., Ho, C. H. & Kim, J. Space observations of cold-cloud phase change. *Proc. Natl Acad. Sci. USA* **107**, 11211–11216 (2010).
160. Stevens, R. G. et al. A model intercomparison of CCN-limited tenuous clouds in the high Arctic. *Atmos. Chem. Phys.* **18**, 11041–11071 (2018).
161. Lohmann, U. A glaciation indirect aerosol effect caused by soot aerosols. *Geophys. Res. Lett.* <https://doi.org/10.1029/2001GL014357> (2002).
162. Vergara-Temprado, J. et al. Strong control of Southern Ocean cloud reflectivity by ice-nucleating particles. *Proc. Natl Acad. Sci. USA* **115**, 2687–2692 (2018).
163. Glassmeier, F. & Lohmann, U. Precipitation susceptibility and aerosol buffering of warm- and mixed-phase orographic clouds in idealized simulations. *J. Atmos. Sci.* **75**, 1173–1194 (2018).
164. French, J. R. et al. Precipitation formation from orographic cloud seeding. *Proc. Natl Acad. Sci. USA* **115**, 1168–1173 (2018).
165. National Research Council. *Critical Issues In Weather Modification Research* (National Academies Press, 2003).
166. Benjamins, Y. et al. The Israel 4 cloud seeding experiment: primary results. *J. Appl. Meteorol. Climatol.* **62**, 317–327 (2023).
167. Korolev, A. & Leisner, T. Review of experimental studies of secondary ice production. *Atmos. Chem. Phys.* **20**, 11767–11797 (2020).
168. Khain, A. P. Notes on state-of-the-art investigations of aerosol effects on precipitation: a critical review. *Environ. Res. Lett.* <https://doi.org/10.1088/1748-9326/4/1/015004> (2009).
169. Miltenberger, A. K., Field, P. R., Hill, A. A., Shipway, B. J. & Wilkinson, J. M. Aerosol–cloud interactions in mixed-phase convective clouds—part 2: meteorological ensemble. *Atmos. Chem. Phys.* **18**, 10593–10613 (2018).
170. Schutgens, N. et al. On the spatio-temporal representativeness of observations. *Atmos. Chem. Phys.* **17**, 9761–9780 (2017).
171. Liu, H. et al. Non-monotonic aerosol effect on precipitation in convective clouds over tropical oceans. *Sci. Rep.* **9**, 7809 (2019).
172. Quaas, J., Stevens, B., Stier, P. & Lohmann, U. Interpreting the cloud cover–aerosol optical depth relationship found in satellite data using a general circulation model. *Atmos. Chem. Phys.* **10**, 6129–6135 (2010).
173. Textor, C. et al. The effect of harmonized emissions on aerosol properties in global models—an AeroCom experiment. *Atmos. Chem. Phys.* **7**, 4489–4501 (2007).
174. Stier, P. Limitations of passive satellite remote sensing to constrain global cloud condensation nuclei. *Atmos. Chem. Phys.* **15**, 32607–32637 (2015).
175. Grandey, B. S., Gururaj, A., Stier, P. & Wagner, T. M. Rainfall–aerosol relationships explained by wet scavenging and humidity. *Geophys. Res. Lett.* **41**, 5678–5684 (2014).
176. Gryspeerdt, E., Stier, P., White, B. A. & Kipling, Z. Wet scavenging limits the detection of aerosol effects on precipitation. *Atmos. Chem. Phys.* **15**, 7557–7570 (2015).
177. Gryspeerdt, E. & Stier, P. Regime-based analysis of aerosol–cloud interactions. *Geophys. Res. Lett.* <https://doi.org/10.1029/2012gl053221> (2012).
178. Gryspeerdt, E., Stier, P. & Partridge, D. G. Links between satellite-retrieved aerosol and precipitation. *Atmos. Chem. Phys.* **14**, 9677–9694 (2014).
179. Storer, R. L., van den Heever, S. C. & L’Ecuyer, T. S. Observations of aerosol-induced convective invigoration in the tropical east Atlantic. *J. Geophys. Res. Atmos.* **119**, 3963–3975 (2014).
180. Berg, W., L’Ecuyer, T. & van den Heever, S. Evidence for the impact of aerosols on the onset and microphysical properties of rainfall from a combination of satellite observations and cloud-resolving model simulations. *J. Geophys. Res. Atmos.* <https://doi.org/10.1029/2007JD009649> (2008).
181. Christensen, M. W. et al. Opportunistic experiments to constrain aerosol effective radiative forcing. *Atmos. Chem. Phys.* **22**, 641–674 (2022).
182. Coakley, J. A., Bernstein, R. L. & Durkee, P. A. Effect of ship-stack effluents on cloud reflectivity. *Science* **237**, 1020–1022 (1987).
183. Christensen, M. W., Coakley, J. A. & Tahnk, W. R. Morning-to-afternoon evolution of marine stratus polluted by underlying ships: implications for the relative lifetimes of polluted and unpolluted clouds. *J. Atmos. Sci.* **66**, 2097–2106 (2009).
184. Manshausen, P., Watson-Parris, D., Christensen, M. W., Jalkanen, J.-P. & Stier, P. Invisible ship tracks show large cloud sensitivity to aerosol. *Nature* **610**, 101–106 (2022).
185. Suzuki, K., Stephens, G. L., Heever, S. C. V. D. & Nakajima, T. Y. Diagnosis of the warm rain process in cloud-resolving models using joint CloudSat and MODIS observations. *J. Atmos. Sci.* **68**, 2655–2670 (2011).
186. Thornton, J. A., Virts, K. S., Holzworth, R. H. & Mitchell, T. P. Lighting enhancement over major oceanic shipping lanes. *Geophys. Res. Lett.* **44**, 9102–9111 (2017).
187. Blosssey, P. N., Bretherton, C. S., Thornton, J. A. & Virts, K. S. Locally enhanced aerosols over a shipping lane produce convective invigoration but weak overall indirect effects in cloud-resolving simulations. *Geophys. Res. Lett.* **45**, 9305–9313 (2018).
188. Berg, W., L’Ecuyer, T. & Kummerow, C. Rainfall climate regimes: the relationship of regional TRMM rainfall biases to the environment. *J. Appl. Meteorol. Climatol.* **45**, 434–454 (2006).
189. Hegerl, G. C. et al. Challenges in quantifying changes in the global water cycle. *Bull. Am. Meteorol. Soc.* **96**, 1097–1115 (2015).

190. Polson, D., Bollasina, M., Hegerl, G. C. & Wilcox, L. J. Decreased monsoon precipitation in the Northern Hemisphere due to anthropogenic aerosols. *Geophys. Res. Lett.* **41**, 6023–6029 (2014).
191. Sarojini, B. B., Stott, P. A. & Black, E. Detection and attribution of human influence on regional precipitation. *Nat. Clim. Change* **6**, 669–675 (2016).
192. Paik, S. et al. Determining the anthropogenic greenhouse gas contribution to the observed intensification of extreme precipitation. *Geophys. Res. Lett.* **47**, e2019GL086875 (2020).
193. Wilcox, L. J., Dong, B., Sutton, R. T. & Highwood, E. J. The 2014 hot, dry summer in Northeast Asia. *Bull. Am. Meteorol. Soc.* **96**, S105–S110 (2015).
194. Wilcox, L. J. et al. Accelerated increases in global and Asian summer monsoon precipitation from future aerosol reductions. *Atmos. Chem. Phys.* **20**, 11955–11977 (2020).
195. Deser, C. et al. Isolating the evolving contributions of anthropogenic aerosols and greenhouse gases: a new CESM1 large ensemble community resource. *J. Clim.* **33**, 7835–7858 (2020).
196. Reddington, C. et al. The Global Aerosol Synthesis and Science Project (GASSP): observations and modelling to reduce uncertainty. *Bull. Am. Meteorol. Soc.* **98**, 1857–1877 (2017).
197. Kahn, R. A. et al. SAM-CAAM: a concept for acquiring systematic aircraft measurements to characterize aerosol air masses. *Bull. Am. Meteorol. Soc.* **98**, 2215–2228 (2017).
198. Wehr, T. et al. The EarthCARE mission — science and system overview. *Atmos. Meas. Tech.* **16**, 3581–3608 (2023).
199. Medeiros, B. Aquaplanets as a framework for examination of aerosol effects. *J. Adv. Model. Earth Syst.* <https://doi.org/10.1029/2019MS001874> (2020).
200. Dingley, B., Dagan, G. & Stier, P. Forcing convection to aggregate using diabatic heating perturbations. *J. Adv. Model. Earth Syst.* <https://doi.org/10.1029/2021MS002579> (2021).
201. Stevens, B. et al. DYAMOND: the dynamics of the atmospheric general circulation modeled on non-hydrostatic domains. *Prog. Earth Planet. Sci.* **6**, 61 (2019).
202. Bauer, P., Stevens, B. & Hazeleger, W. A digital twin of Earth for the green transition. *Nat. Clim. Change* **11**, 80–83 (2021).
203. Gillett, N. P. et al. The Detection and Attribution Model Intercomparison Project (DAMIP v1.0) contribution to CMIP6. *Geosci. Model Dev.* **9**, 3685–3697 (2016).
204. Giorgetta, M. A. et al. ICON-A, the atmosphere component of the ICON Earth system model: I. Model description. *J. Adv. Model. Earth Syst.* **10**, 1613–1637 (2018).

## Acknowledgements

This review builds on an expert workshop of the Global Energy and Water Cycle Exchanges (GEWEX) Aerosol Precipitation (GAP) initiative hosted by the University of Oxford with support of the European Research Council (ERC) project Constraining the Effects of Aerosols on Precipitation (RECAP) under the European Union's Horizon 2020 research and innovation programme with grant agreement no. 724602. P.S. acknowledges support by the Alexander von Humboldt Foundation. S.C.v.d.H. acknowledges support from NASA grant 80NSSC18K0149. A.M.L.E., U.L., J.Q. and P.S. acknowledge funding by the FORCeS project under the European

Union's Horizon 2020 research programme with grant agreement 821205. J.Q. acknowledges funding by the BMBF project PATTERN (FKZ 01LP1902C). G.M. acknowledges support from the Research Council of Norway project SUPER (no. 250573). E.G. was supported by a Royal Society University Research Fellowship (URF/R1/191602). S.M.S. was supported by the US Department of Energy Atmospheric System Research grant no. DE-SC0021160. K.E. was supported by the National Science Foundation under grant AGS-1906768. M.W.C. acknowledges support from the Pacific Northwest National Laboratory operated for the US Department of Energy by Battelle Memorial Institute under contract no. DE-AC05-76RL01830. We thank D. Watson-Parris for providing CMIP6 precipitation data and helpful feedback. We acknowledge the World Climate Research Programme, which, through its Working Group on Coupled Modelling, coordinated and promoted CMIP6 and thank the modelling groups for making available their model output, the Earth System Grid Federation (ESGF) for archiving and providing access, and multiple funding agencies supporting CMIP6 and ESGF.

## Author contributions

P.S. and S.C.v.d.H. developed the structure of the GEWEX Aerosol Precipitation Initiative workshop programme providing the basis for this review paper. M.W.C. and E.G. served as rapporteurs providing detailed meeting notes. P.S. and S.C.v.d.H. drafted the first version of the manuscript that was extended with contributions from M.W.C., E.G., G.D., M.B., L.D., K.E., A.M.L.E., G.F., P. Field, P. Forster, J.H., R.K., I.K., C.K., T.L., U.L., Y.M., G.M., J.Q., D.R., B.S., A.S., G.S. and W.-K.T. to the literature review, the synthesis of the results and the revised manuscript. G.D. created Figs. 1 and 3. P.S. created Fig. 2. S.M.S. created Fig. 4.

## Competing interests

The authors declare no competing interests.

## Additional information

**Correspondence and requests for materials** should be addressed to Philip Stier or Susan C. van den Heever.

**Peer review information** *Nature Geoscience* thanks Pier Luigi Vidale and the other, anonymous, reviewer(s) for their contribution to the peer review of this work. Primary Handling Editor: James Super, in collaboration with the *Nature Geoscience* team.

**Reprints and permissions information** is available at [www.nature.com/reprints](http://www.nature.com/reprints).

**Publisher's note** Springer Nature remains neutral with regard to jurisdictional claims in published maps and institutional affiliations.

Springer Nature or its licensor (e.g. a society or other partner) holds exclusive rights to this article under a publishing agreement with the author(s) or other rightsholder(s); author self-archiving of the accepted manuscript version of this article is solely governed by the terms of such publishing agreement and applicable law.

© Springer Nature Limited 2024

<sup>1</sup>Department of Physics, University of Oxford, Oxford, UK. <sup>2</sup>Department of Atmospheric Science, Colorado State University, Fort Collins, CO, USA.

<sup>3</sup>Pacific Northwest National Laboratory, Richland, WA, USA. <sup>4</sup>Space and Atmospheric Physics Group, Imperial College London, London, UK.

<sup>5</sup>Institute of Earth Sciences, The Hebrew University of Jerusalem, Jerusalem, Israel. <sup>6</sup>School of GeoSciences, Grant Institute, The University of Edinburgh, Edinburgh, UK. <sup>7</sup>NOAA/GFDL, Princeton University Forrestal Campus, Princeton, NJ, USA. <sup>8</sup>Lorenz Center, Massachusetts Institute of Technology, Cambridge, MA, USA. <sup>9</sup>Department of Meteorology and Bolin Centre for Climate Research, Stockholm University, Stockholm, Sweden. <sup>10</sup>Laboratory for Atmospheric and Space Physics, University of Colorado, Boulder, CO, USA. <sup>11</sup>School of Earth and Environment, University of Leeds, Leeds, UK.

<sup>12</sup>Met Office, Exeter, UK. <sup>13</sup>Priestley International Centre for Climate, University of Leeds, Leeds, UK. <sup>14</sup>Department of Mathematics and Statistics,

Faculty of Environment, Science and Economy, University of Exeter, Exeter, UK. <sup>15</sup>NASA Goddard Space Flight Center, Greenbelt, MD, USA.

<sup>16</sup>Department of Earth and Planetary Sciences, Weizmann Institute of Science, Rehovot, Israel. <sup>17</sup>Department of Atmospheric and Oceanic Sciences, University of Wisconsin, Madison, WI, USA. <sup>18</sup>Institute for Atmospheric and Climate Science, ETH Zürich, Zürich, Switzerland. <sup>19</sup>Department of Earth and Environmental Sciences, Boston College, Chestnut Hill, MA, USA. <sup>20</sup>Center for International Climate Research, Oslo, Norway. <sup>21</sup>Institute for Meteorology, Leipzig University, Leipzig, Germany. <sup>22</sup>Deutscher Wetterdienst, Offenbach, Germany. <sup>23</sup>Jet Propulsion Laboratory, California Institute of Technology, Pasadena, CA, USA. <sup>24</sup>Mesoscale Atmospheric Processes Laboratory, NASA/Goddard Space Flight Center, Greenbelt, MD, USA.

✉ e-mail: [philip.stier@physics.ox.ac.uk](mailto:philip.stier@physics.ox.ac.uk); [Sue.vandenHeever@colostate.edu](mailto:Sue.vandenHeever@colostate.edu)